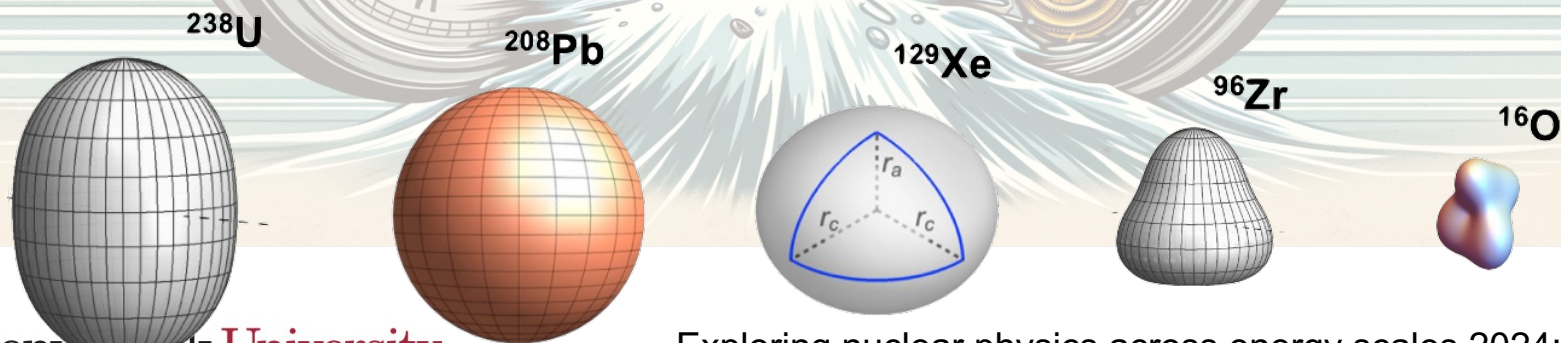


Probe structure of nuclei available at colliders

Jiangyong Jia

April 16, 2024



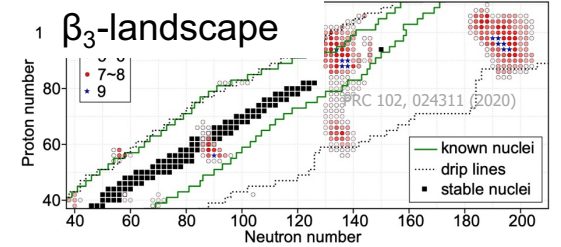
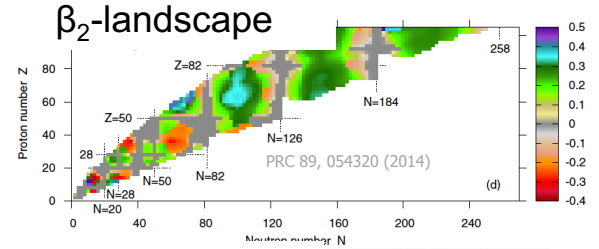
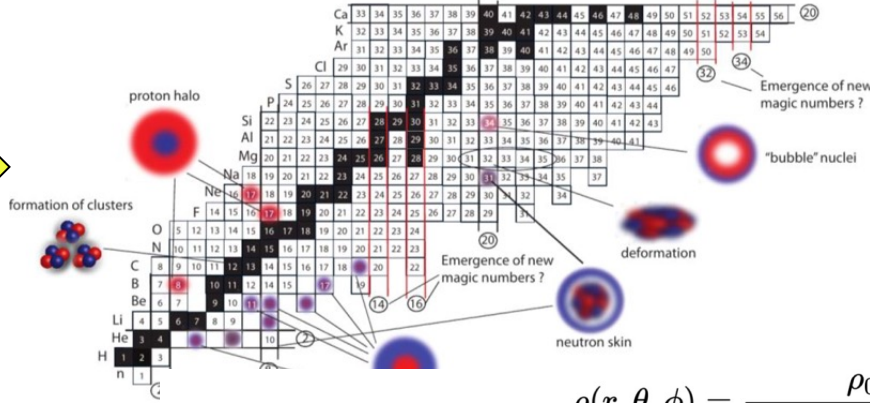
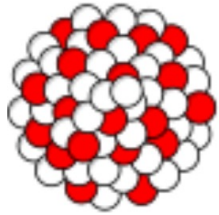
Stony Brook University

Exploring nuclear physics across energy scales 2024:
intersection between nuclear structure and high energy nuclear collisions

Atomic nuclei and their shapes

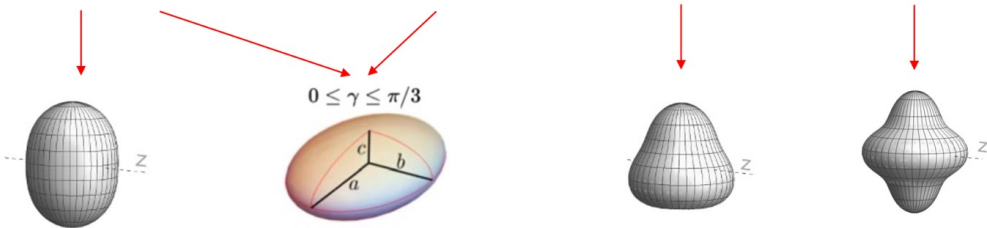
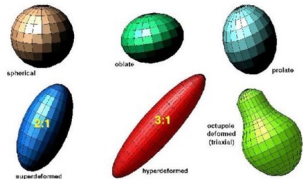
Emergent phenomena of a many-body quantum system

- clustering, halo, skin, bubble...
- quadrupole/octupole/hexadecapole deformations
- Non-monotonic evolution with N and Z



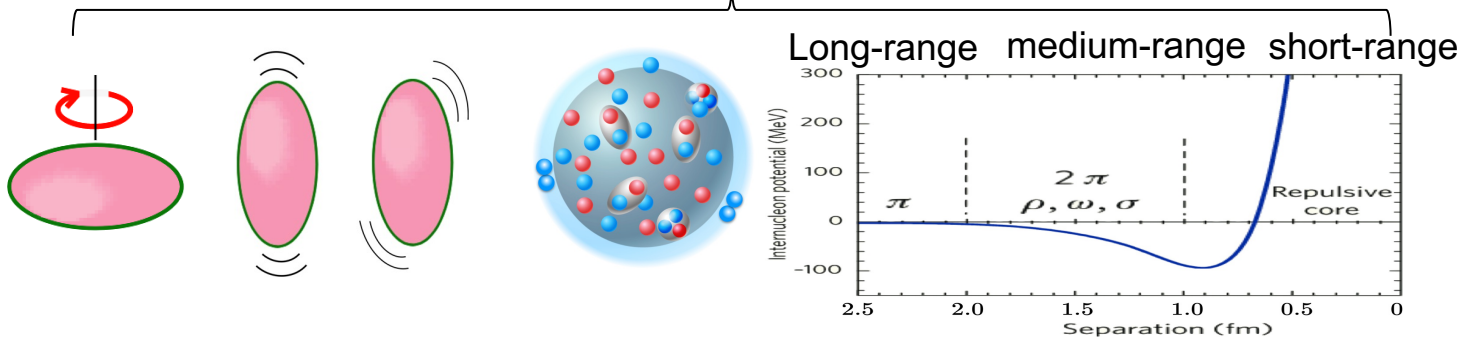
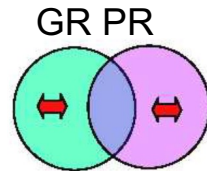
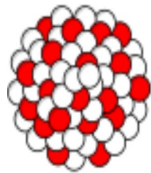
$$\rho(r, \theta, \phi) = \frac{\rho_0}{1 + e^{(r-R(\theta, \phi))/a_0}}$$

$$R(\theta, \phi) = R_0(1 + \beta_2[\cos \gamma Y_{2,0}(\theta, \phi) + \sin \gamma Y_{2,2}(\theta, \phi)] + \beta_3 Y_{3,0}(\theta, \phi) + \beta_4 Y_{4,0}(\theta, \phi))$$



Degrees-of-freedom and timescales

Heavy nuclei



$$E = \frac{p^2}{2m}$$

Energy scales:
(MeV)

rotation

~0.04

vibration

~0.5-2

clustering

~a few

nucleon correlations

~1-50



resonances
quarks,
gluons

Timescales:
(fm/c)

10^4 - 10^3

~1000

~1000-100

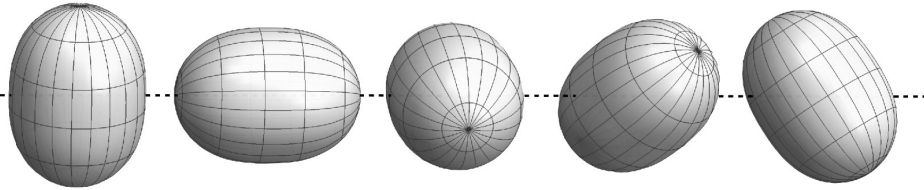
~100 to a few

$$\hbar = 197\text{MeV} \times \frac{\text{fm}}{c}$$

Nuclear shape in low-energy methods

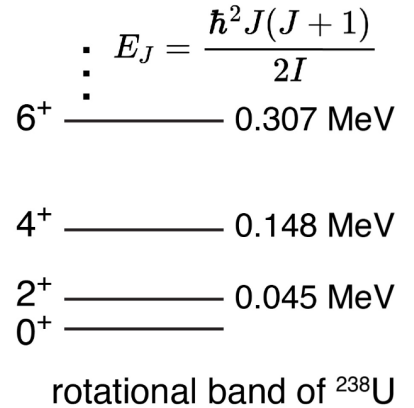
Each DOF has zero-point fluctuations within an intrinsic timescale.

quantum fluctuations in orientations



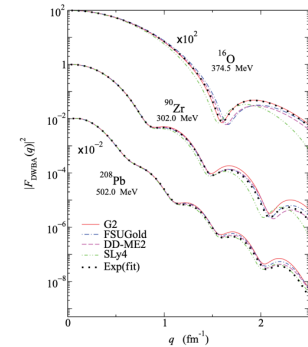
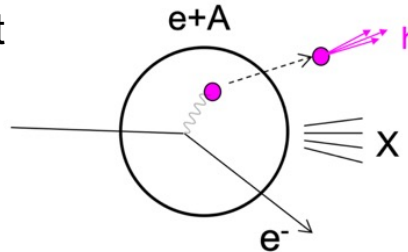
time scale: $\tau \gtrsim I/\hbar \sim 10^3 - 10^4 \text{ fm}/c$

wavefunctions probed in spectroscopy method



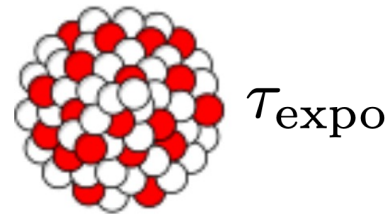
(non-invasive) spectroscopic methods probe a superposition of these fluctuations
 Instantaneous nuclear shapes are not directly seen → intrinsic shape not observable

e+A scattering has very short timescales, but so far mostly imaged the one-body (charge) distribution. The impact of deformation appears as an increase in the radius



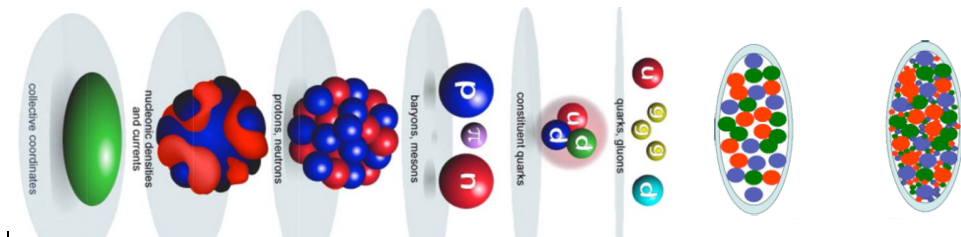
Taking a snapshot

To see event-by-event shape directly, one must have access to instantaneous many-body distribution $\rho(\mathbf{r}_1, \mathbf{r}_2 \dots)$

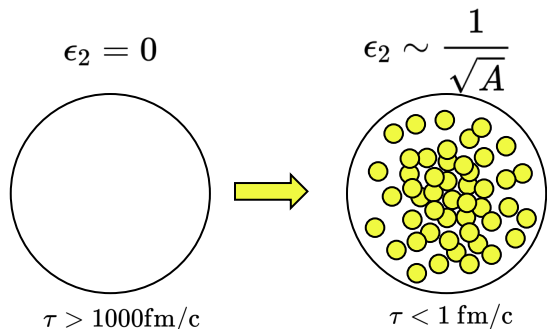


But we will see all DOFs longer than this timescale: $\tau > \tau_{expo}$

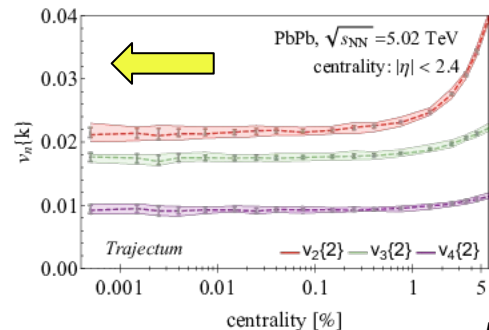
Nucleons, hadrons, quark, gluons, gluon saturations



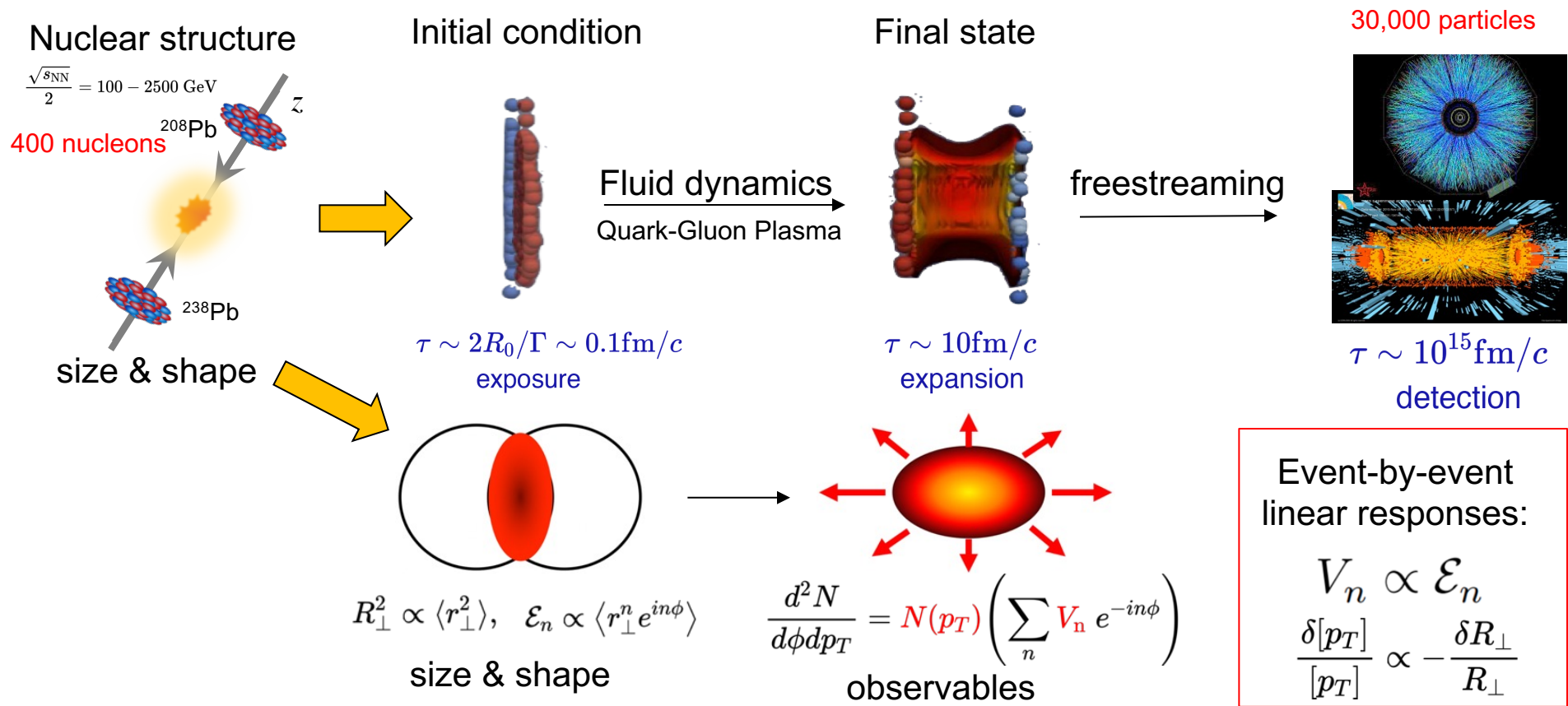
The concept of shape in principle collision energy dependent



$$\epsilon_2 = \underbrace{\epsilon_0}_{\sqrt{s}\text{-dependent fluctuations}} + \underbrace{\mathbf{p}(\Omega)\beta_2}_{\text{Global shape vibrational}} + \mathcal{O}(\beta_2^2)$$



Flow-assisted nuclear shape imaging at high-energy



Key: 1) fast snapshot, 2) linear response, 3) large multiplicity for many-body correlations

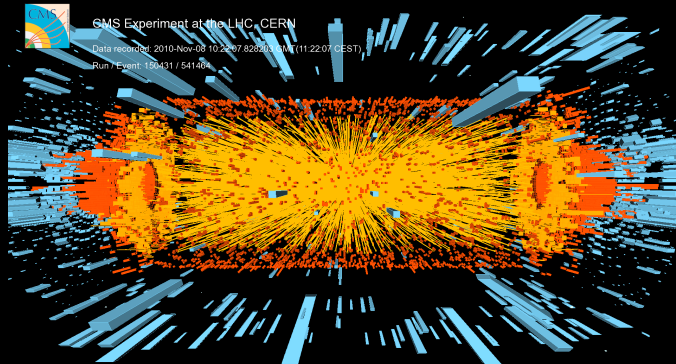
Seen by ATLAS detector



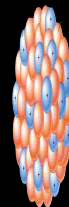
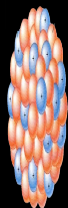
CMS Experiment at the LHC, CERN

Data recorded: 2010-Nov-08 10:22:07.82831000 (11:22:07.82831000)

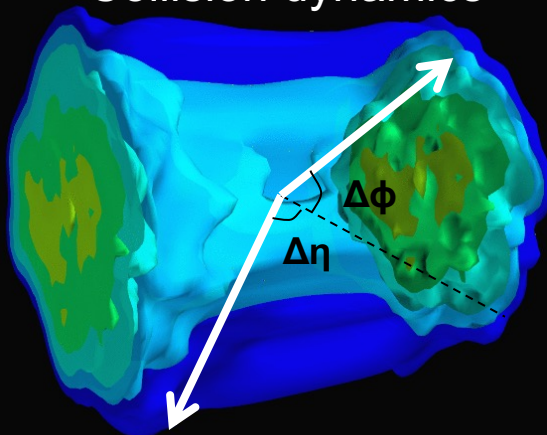
Run / Event: 120431 / 54140



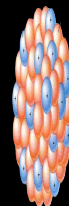
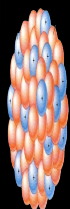
$t \sim 10^{-8} \text{ s}$



Collision dynamics



$t \sim 10 \text{ fm}/c = 10^{-22} \text{ s}$



3D relativistic viscous hydrodynamics

Credit: Bjoern Schenke

Hydrodynamic EFT

Energy-momentum conservation

$$\partial_\mu T^{\mu\nu} = 0$$

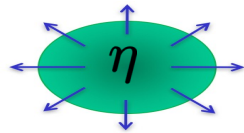
Relativistic viscous Hydrodynamics (first-order):

$$T^{\mu\nu} = \underbrace{\epsilon u^\mu u^\nu}_{\text{Equation-of-state } P(\epsilon)} - \underbrace{(P + \Pi)}_{\text{Bulk pressure}} \Delta^{\mu\nu} + \underbrace{\pi^{\mu\nu}}_{\text{Shear tensor}}$$

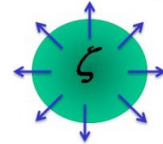
$$\pi^{\mu\nu} = -\eta \sigma^{\mu\nu} \quad \eta: \text{shear viscosity} \quad \Pi = -\zeta \nabla_\lambda^\perp u^\lambda \quad \zeta: \text{bulk viscosity}$$

1) Collective flow driven by QCD eos: $F = -\nabla P(\epsilon)$

2) But resisted by viscosity

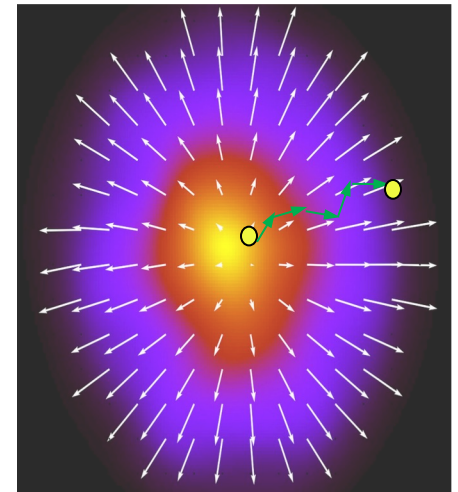


Reduce anisotropic flow



Reduce radial flow

Valid when mean free path \ll system size 



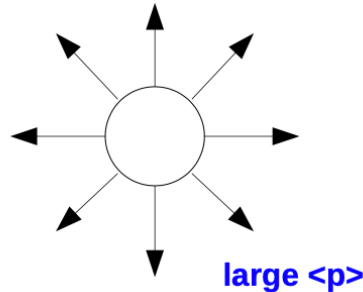
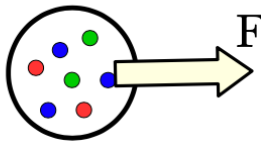
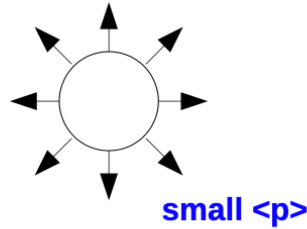
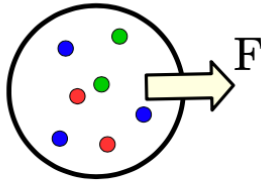
Initial geometry to Collective flow

Shape-flow transmutation via pressure-gradient force: $F = -\nabla P(\epsilon)$

$$\frac{\delta[p_T]}{[p_T]} \propto -\frac{\delta R_\perp}{R_\perp} \quad \frac{d^2 N}{d\phi dp_T} = N(p_T) \left(\sum_n V_n e^{-in\phi} \right) \quad V_n \propto \mathcal{E}_n$$

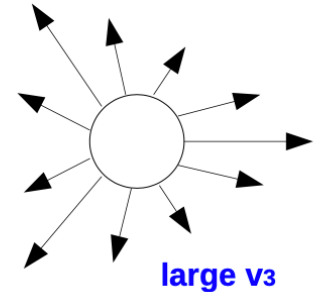
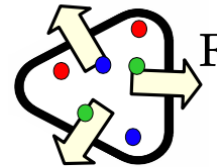
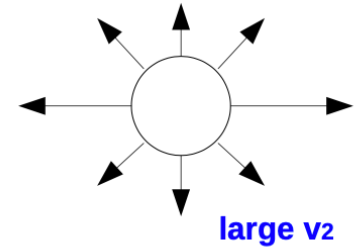
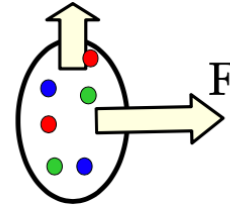
initial state (x)

final state (p)



initial state (x)

final state (p)



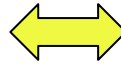
Accessing information in intrinsic frame

$$\mathcal{E}_2 \equiv \varepsilon_2 e^{2i\Phi_2} \propto \int_{\mathbf{r}} \mathbf{r}^2 \rho(\mathbf{r})$$

$$d_{\perp} = 1/R_{\perp} \quad \delta d_{\perp} = d_{\perp} - \langle d_{\perp} \rangle$$

- We measure moments of $p(1/R, \varepsilon_2, \varepsilon_3 \dots)$ via $p([p_T], v_2, v_3 \dots)$...

■ Mean	$\langle d_{\perp} \rangle$	$\langle p_T \rangle$
■ Variance:	$\langle \varepsilon_n^2 \rangle, \langle (\delta d_{\perp}/d_{\perp})^2 \rangle$	$\langle v_n^2 \rangle, \langle (\delta p_T/p_T)^2 \rangle$
■ Skewness	$\langle \varepsilon_n^2 \delta d_{\perp}/d_{\perp} \rangle, \langle (\delta d_{\perp}/d_{\perp})^3 \rangle$	$\langle v_n^2 \delta p_T/p_T \rangle, \langle (\delta p_T/p_T)^3 \rangle$
■ Kurtosis	$\langle \varepsilon_n^4 \rangle - 2\langle \varepsilon_n^2 \rangle^2, \langle (\delta d_{\perp}/d_{\perp})^4 \rangle - 3\langle (\delta d_{\perp}/d_{\perp})^2 \rangle^2$	$\langle v_n^4 \rangle - 2\langle v_n^2 \rangle^2, \langle (\delta p_T/p_T)^4 \rangle - 3\langle (\delta p_T/p_T)^2 \rangle^2$
...		



- Higher moments probe the frame-independent many-body distributions 1902.07168

$$\langle \varepsilon_2^2 \rangle = \langle \mathcal{E}_2 \mathcal{E}_2^* \rangle \approx \frac{\int_{\mathbf{r}_1, \mathbf{r}_2} (\mathbf{r}_1)^2 (\mathbf{r}_2^*)^2 \rho(\mathbf{r}_1, \mathbf{r}_2)}{(\int_{\mathbf{r}} |\mathbf{r}|^2 \langle \rho(\mathbf{r}) \rangle)^2}$$

$$\langle \varepsilon_2^2 \delta d_{\perp}/d_{\perp} \rangle \approx - \frac{\int_{\mathbf{r}_1, \mathbf{r}_2, \mathbf{r}_3} (\mathbf{r}_1)^2 (\mathbf{r}_2^*)^2 |\mathbf{r}_3|^2 \rho(\mathbf{r}_1, \mathbf{r}_2, \mathbf{r}_3)}{(\int_{\mathbf{r}} |\mathbf{r}|^2 \langle \rho(\mathbf{r}) \rangle)^2 \int_{\mathbf{r}} |\mathbf{r}|^2 \langle \rho(\mathbf{r}) \rangle}$$

$$\rho(\mathbf{r}_1, \mathbf{r}_2) = \langle \delta \rho(\mathbf{r}_1) \delta \rho(\mathbf{r}_2) \rangle = \langle \rho(\mathbf{r}_1) \rho(\mathbf{r}_2) \rangle - \langle \rho(\mathbf{r}_1) \rangle \langle \rho(\mathbf{r}_2) \rangle$$

$$\rho(\mathbf{r}_1, \mathbf{r}_2, \mathbf{r}_3) = \langle \delta \rho(\mathbf{r}_1) \delta \rho(\mathbf{r}_2) \delta \rho(\mathbf{r}_3) \rangle$$

Coulomb Explosion Imaging in Chemistry

Instantaneous stripping of electrons (thin foil or x-ray laser), and then let atoms explode under mutual coulomb repulsion

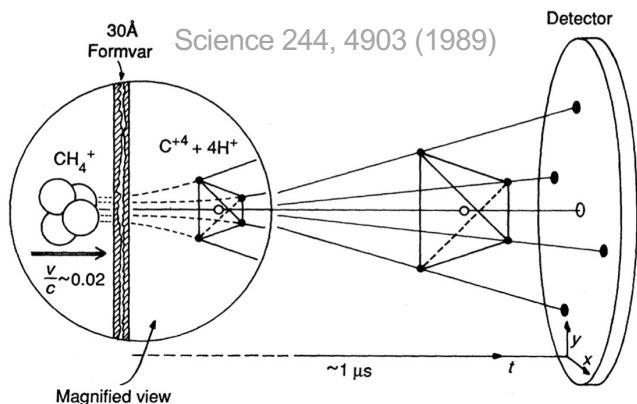
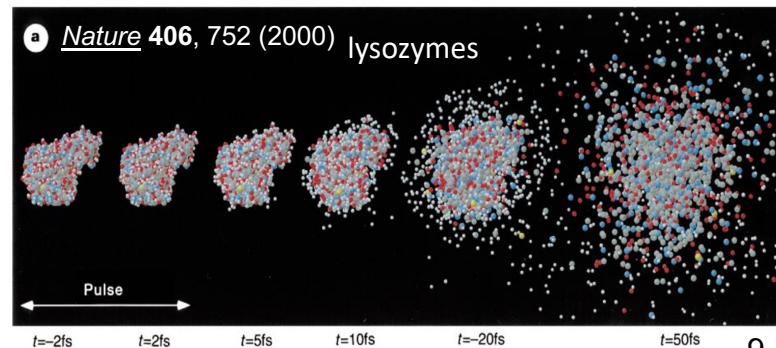
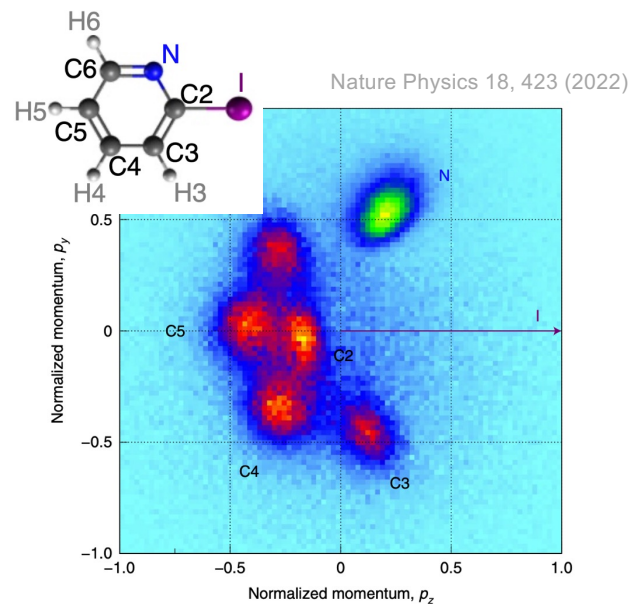


Fig. 1. A schematic view of a Coulomb explosion experiment. When a swift molecule passes through a thin solid film, it loses all of its binding electrons. The remaining positive ions repel each other, thus transforming the microstructure (as seen in the magnified view) into a macrostructure that can be measured precisely with an appropriate detector. The measured traces (x , y , t) of each fragment nucleus for individual molecules are then transformed into the original molecular structure.



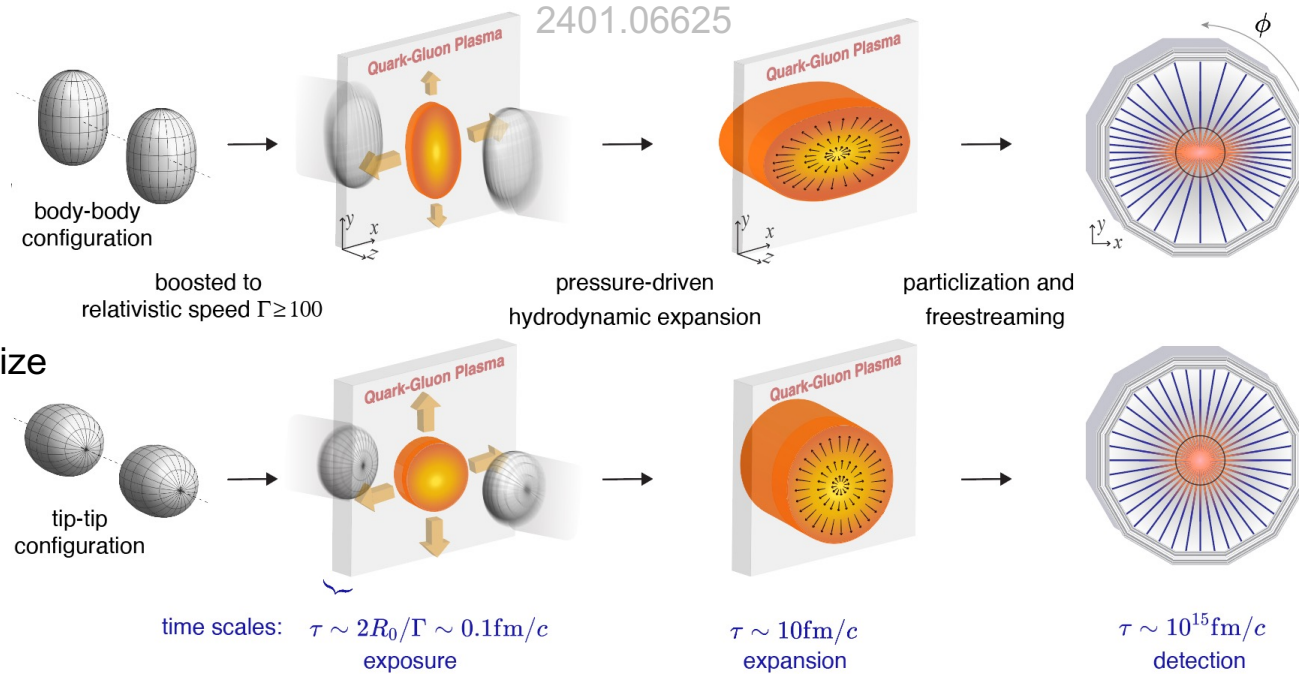
“Nuclear explosion imaging” is 10^6 - 10^9 times faster.

Applications of nuclear structure imaging

- Demonstration of methodology → deformation of Uranium238
- Layout the general strategy of structure imaging
- Establishing the precision via isobar collisions: $^{96}\text{Ru}+^{96}\text{Ru}$ vs $^{96}\text{Zr}+^{96}\text{Zr}$
- Future opportunities.

Impact of quadrupole deformation in U+U

Collision geometry depends on the orientations: Head-on collisions has two extremes body-body or tip-tip collisions



Body-body: large-eccentricity large-size

$$v_2 \nearrow \quad p_T \searrow$$

Tip-tip : small-eccentricity small-size

$$v_2 \searrow \quad p_T \nearrow$$

$$\langle v_2^2 \rangle = a_1 + b_1 \beta_2^2,$$

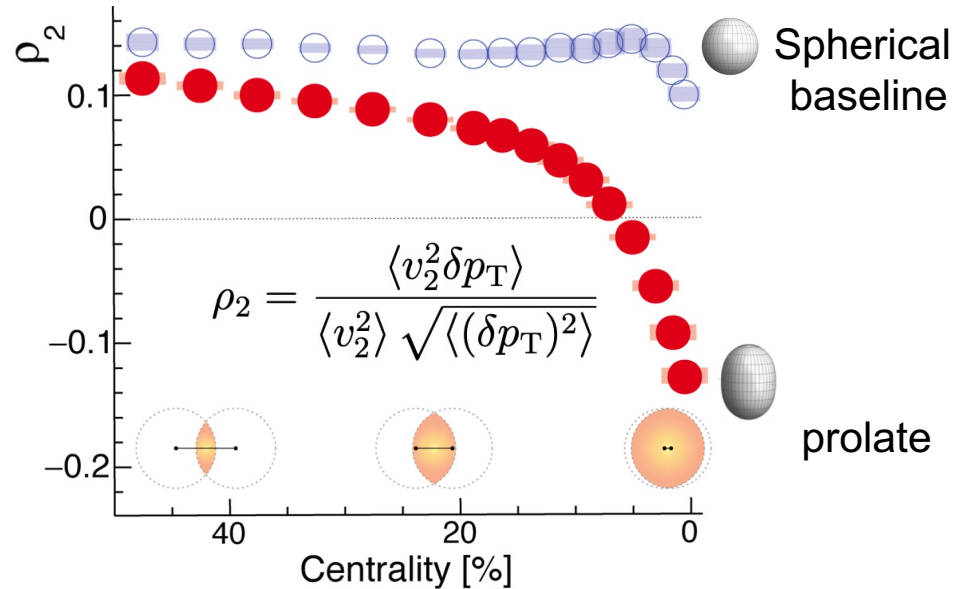
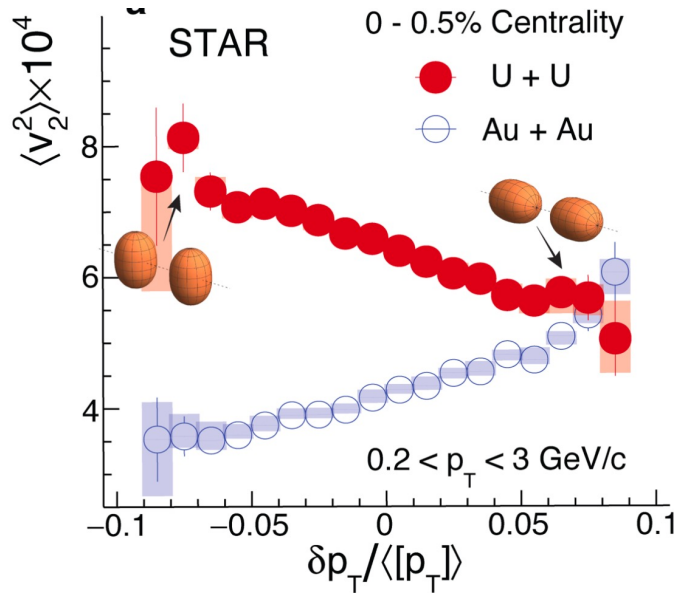
$$\langle (\delta p_T)^2 \rangle = a_2 + b_2 \beta_2^2,$$

$$\langle v_2^2 \delta p_T \rangle = a_3 - b_3 \beta_2^3 \cos(3\gamma)$$

Deformation enhances the fluctuations of v_2 and $[p_T]$.
Also leads to anticorrelation between v_2 and $[p_T]$.

Impact of quadrupole deformation

Seen directly by comparing $^{238}\text{U}+^{238}\text{U}$ with near-spherical $^{197}\text{Au}+^{197}\text{Au}$

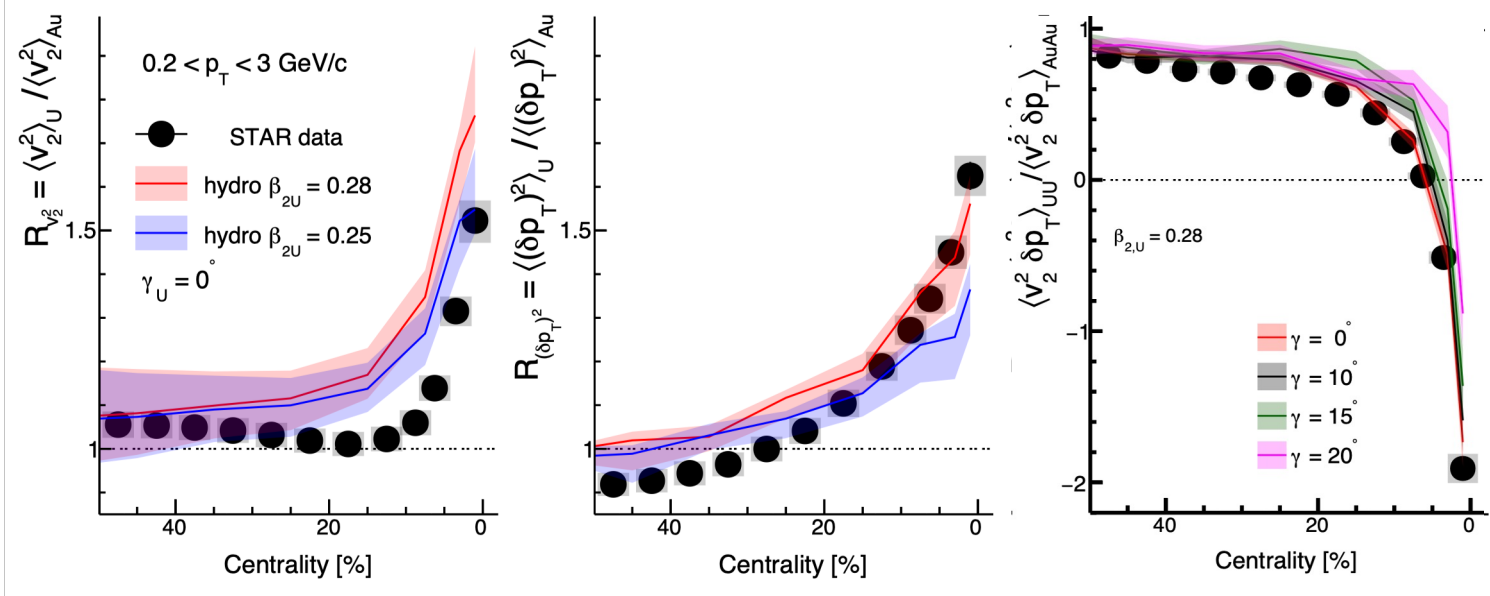


2401.06625

Near-spherical \rightarrow flat ρ_2 vs centrality

Strongly prolate \rightarrow decreasing ρ_2 vs centrality

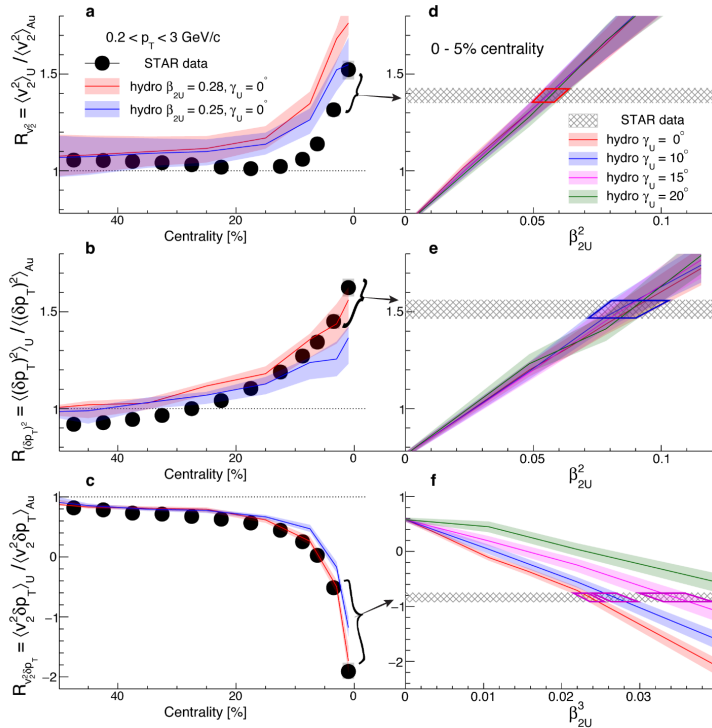
Ratio of observables $R_{\mathcal{O}} = \langle \mathcal{O} \rangle_{U+U} / \langle \mathcal{O} \rangle_{Au+Au}$



Compare with state-of-the-art IPGlasma+Music+UrQMD hydro model 2005.14682

- Increase of $\langle v_2^2 \rangle$ in model is less sharp \rightarrow overestimate ratio of $v_2^{RP} \rightarrow$ lower bound β_{2U} .
- The $\langle (\delta p_T)^2 \rangle$ and $\langle v_2^2 \delta p_T \rangle$ data seem to prefer values close to $\beta_{2U} = 0.28$.
- $\langle v_2^2 \delta p_T \rangle$ has additional sensitivity to $\gamma_U \rightarrow$ simultaneously constrain the β_{2U} and γ_U .

Constraining Uranium shape parameters 2401.06625

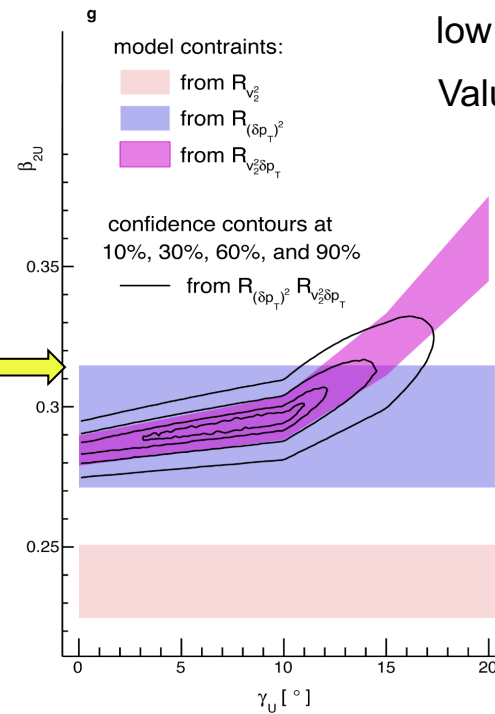


Relations confirmed!

$$\langle v_2^2 \rangle = a_1 + b_1 \beta_2^2,$$

$$\langle (\delta p_T)^2 \rangle = a_2 + b_2 \beta_2^2,$$

$$\langle v_2^2 \delta p_T \rangle = a_3 - b_3 \beta_2^3 \cos(3\gamma)$$



Derive a confidence contour

$$\beta_{2U} = 0.297 \pm 0.013$$

$$\gamma_U = 8.6^\circ \pm 4.8^\circ$$

low energy estimate $\beta_{2U} = 0.287 \pm 0.009$

Value could be smaller due to possible β_4 .

$$\beta_{2U} \sim 0.25 - 0.26 \quad 2302.13617$$

Structure models suggest triaxiality, which seems to be preferred by the HI data.

PRC 54, 2356 (1996)

arXiv:2303.11299

But we cannot distinguish between rigid triaxiality and triaxial fluctuations

This can be done in the future using six-particle correlations: $v_2\{6\}$, $\langle v_2^4 \delta p_T^2 \rangle_c$.

2301.03556

2403.07441

Ratios cancel final state effects

- Vary the shear/bulk viscosity in Music hydro model

- Flow signal change by more than factor of 2, yet the ratio unchanged.

$$v_2 \propto \varepsilon_2$$

$$\delta p_T \propto -\delta R$$

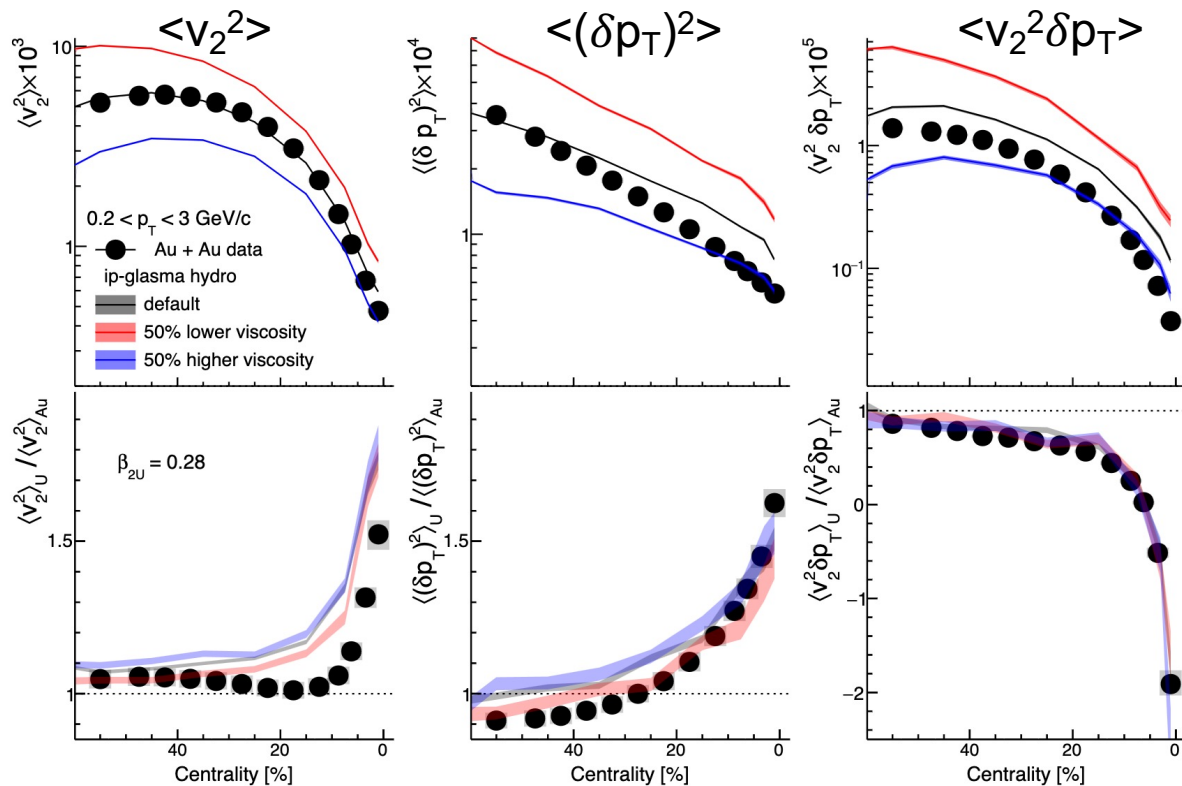


$$\frac{v_{2,U}}{v_{2,Au}} \approx \frac{\varepsilon_{2,U}}{\varepsilon_{2,Au}}$$

$$\frac{\langle (\delta p_T)^2 \rangle_U}{\langle (\delta p_T)^2 \rangle_{Au}} \approx \frac{\langle (\delta R)^2 \rangle_U}{\langle (\delta R)^2 \rangle_{Au}}$$

$$\frac{\langle v_2^2 \delta p_T \rangle_U}{\langle v_2^2 \delta p_T \rangle_{Au}} \approx \frac{\langle \varepsilon_2^2 \delta R \rangle_U}{\langle \varepsilon_2^2 \delta R \rangle_{Au}}$$

Robust probe of
initial state!



A general strategy for nuclear shape imaging

Flow observable = **k** \otimes initial condition (structure)

QGP response,
a smooth function of N+Z

Structure of colliding nuclei,
non-monotonic function of N and Z

Compare two systems of similar mass but different structure

Two-particle observable:
$$R_{\mathcal{O}} \equiv \frac{\mathcal{O}_{Ru}}{\mathcal{O}_{Zr}} \approx 1 + c_1 \Delta\beta_2^2 + c_2 \Delta\beta_3^2 + c_3 \Delta R_0 + c_4 \Delta a$$

Deviation from unity depends only on their structure differences

Available collision systems

Nuclear Structure \leftrightarrow Initial Condition \leftrightarrow QGP dynamics/properties

RHIC $\sqrt{s}=200\text{GeV}$

LHC $\sqrt{s}=5000\text{ GeV}$

$^{197}\text{Au}+^{197}\text{Au}$ vs $^{238}\text{U}+^{238}\text{U}$

$\beta_{2\text{U}}$ γ_{U}
 $\beta_{3\text{U}}$ $\beta_{4\text{U}}$

Establish methodology

- Large sensitivity

$^{129}\text{Xe}+^{129}\text{Xe}$ vs $^{208}\text{Pb}+^{208}\text{Pb}$

$\beta_{2\text{Xe}}$ γ_{Xe}

Neutron skin

See talk of G. Nils, C. Zhang, Y. Zhou, H. Xu

$^{96}\text{Ru}+^{96}\text{Ru}$ vs $^{96}\text{Zr}+^{96}\text{Zr}$

$\beta_{2\text{Ru}}$

$\beta_{3\text{Zr}}$
large skin

Establish precision

- 0.2% measurement error vs 5-15% signal
- High-order observables

See talk of C. Zhang, H. Xu

$\text{d}+^{197}\text{Au}$ vs $^{16}\text{O}+^{16}\text{O}$

Structure of light nuclei

- Cluster, subnucleon structure.
- Benchmark ab-initio models

$^{16}\text{O}+^{16}\text{O}$ vs $^{20}\text{Ne}+^{20}\text{Ne}?$

See talk of G. Giacalone

$\text{p}+\text{p}$, $\text{p}+^{27}\text{Al}$, $\text{p}+^{197}\text{Au}$, $^3\text{He}+^{197}\text{Au}$,
 $^{63}\text{Cu}+^{63}\text{Cu}$, $^{63}\text{Cu}+^{197}\text{Au}$

What can we learn from these?

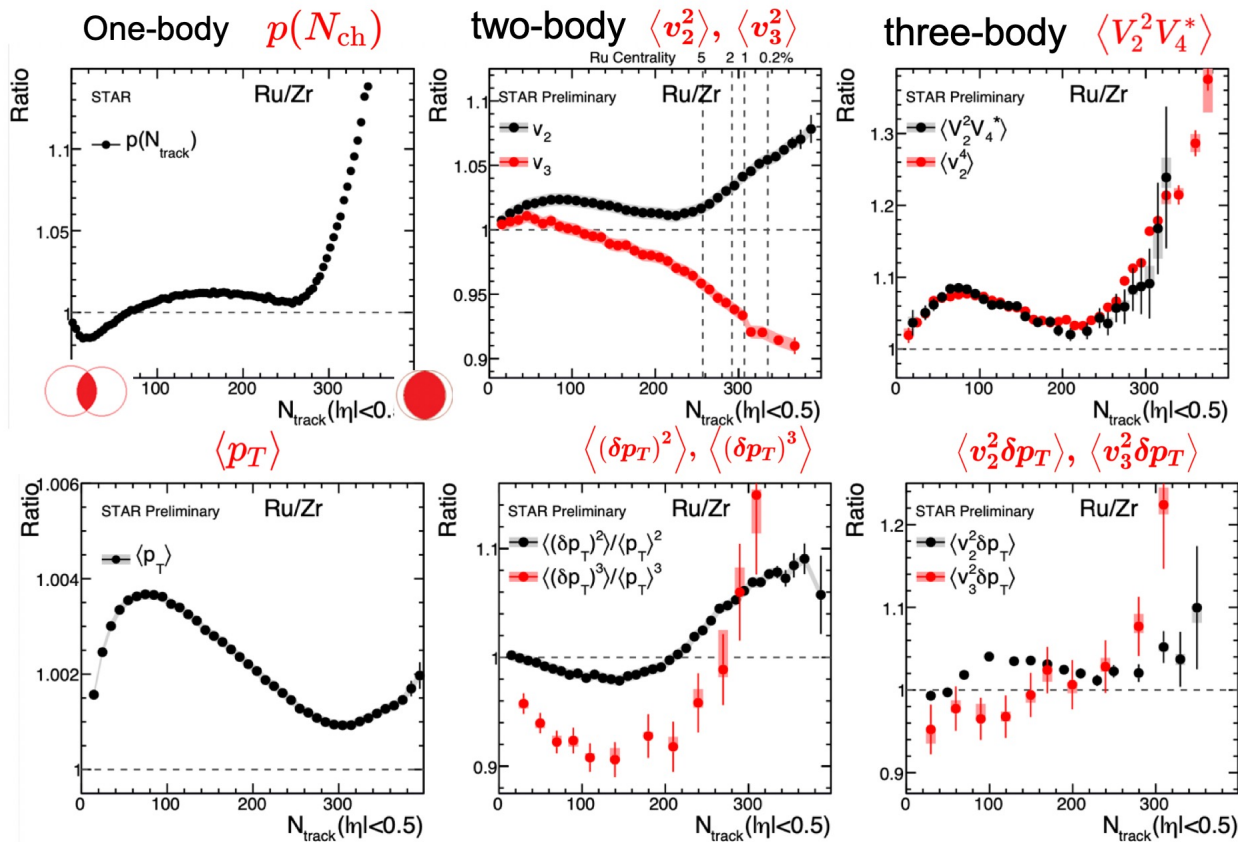
$\text{p}+\text{p}$, $\text{p}+^{16}\text{O}$, $\text{p}+^{208}\text{Pb}$

What interesting species to consider & what questions do they answer?

Isobar $^{96}\text{Ru}+^{96}\text{Ru}$ and $^{96}\text{Zr}+^{96}\text{Zr}$ collisions at RHIC 200 GeV

QM2022 poster, Chunjian Zhang

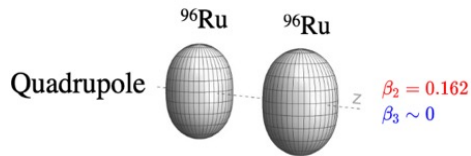
$$R_{\mathcal{O}} \equiv \frac{\mathcal{O}_{\text{Ru}}}{\mathcal{O}_{\text{Zr}}}$$



Structure influences everywhere

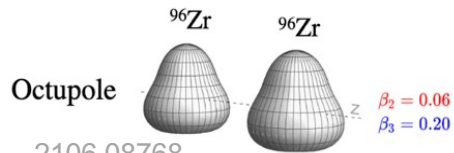
Nuclear structure is inherently part of Heavy ion problem

Nuclear structure via v_2 -ratio and v_3 -ratio



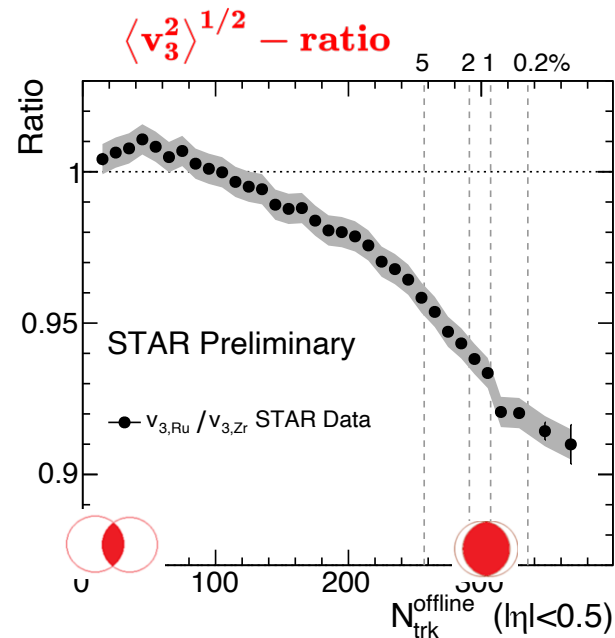
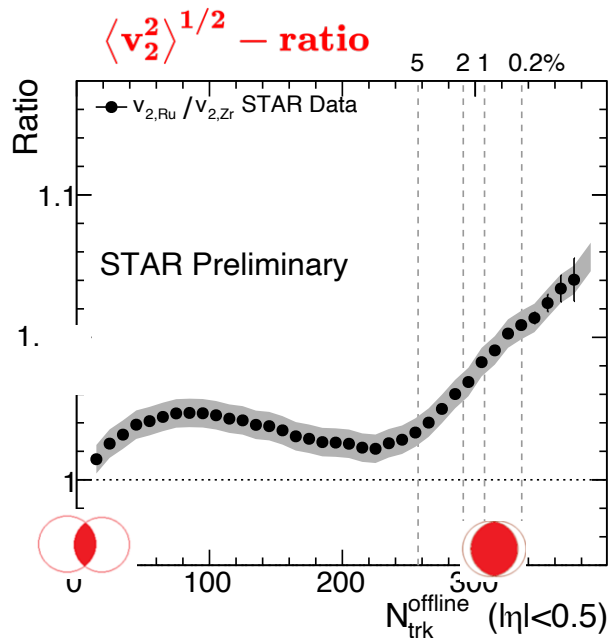
$$R_{\mathcal{O}} \equiv \frac{\mathcal{O}_{\text{Ru}}}{\mathcal{O}_{\text{Zr}}} \approx 1 + c_1 \Delta\beta_2^2 + c_2 \Delta\beta_3^2 + c_3 \Delta R_0 + c_4 \Delta a$$

Simultaneously constrain four structure parameters

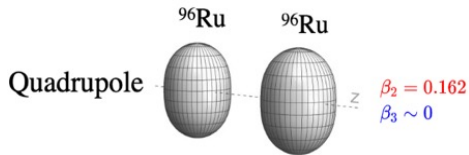


2106.08768

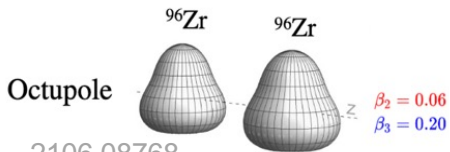
Species	β_2	β_3	a_0	R_0
Ru	0.162	0	0.46 fm	5.09 fm
Zr	0.06	0.20	0.52 fm	5.02 fm
difference	$\Delta\beta_2^2$	$\Delta\beta_3^2$	Δa_0	ΔR_0
	0.0226	-0.04	-0.06 fm	0.07 fm



Nuclear structure via v_2 -ratio and v_3 -ratio



$$R_{\mathcal{O}} \equiv \frac{O_{\text{Ru}}}{O_{\text{Zr}}} \approx 1 + c_1 \Delta\beta_2^2 + c_2 \Delta\beta_3^2 + c_3 \Delta R_0 + c_4 \Delta a$$

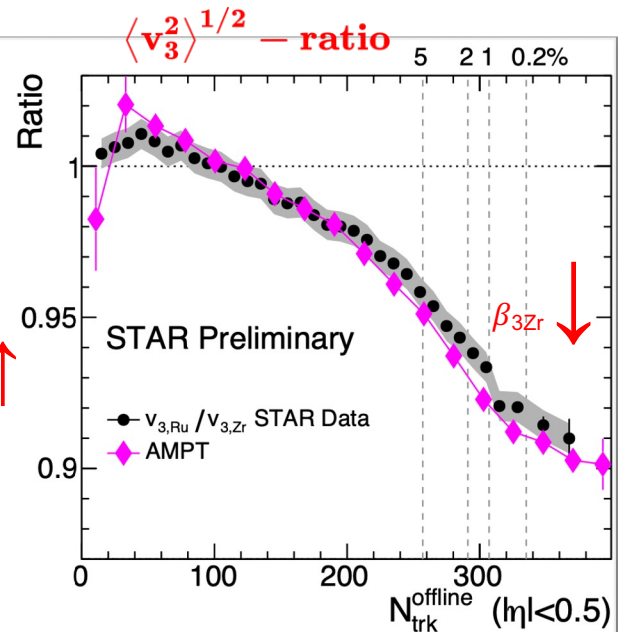
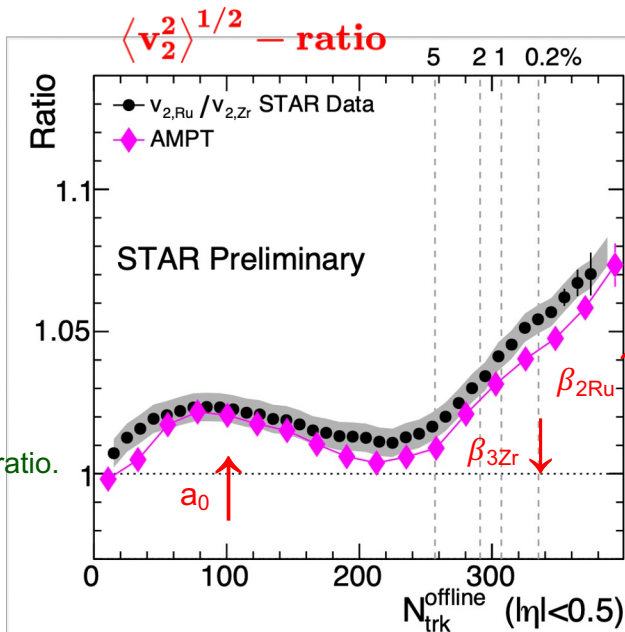


Simultaneously constrain four structure parameters

Species	β_2	β_3	a_0	R_0
Ru	0.162	0	0.46 fm	5.09 fm
Zr	0.06	0.20	0.52 fm	5.02 fm
difference	$\Delta\beta_2^2$	$\Delta\beta_3^2$	Δa_0	ΔR_0
	0.0226	-0.04	-0.06 fm	0.07 fm

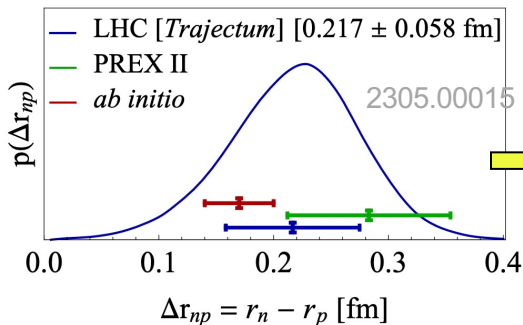
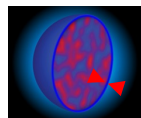
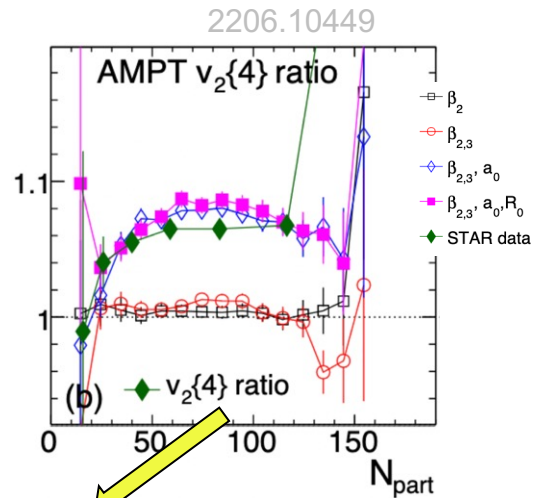
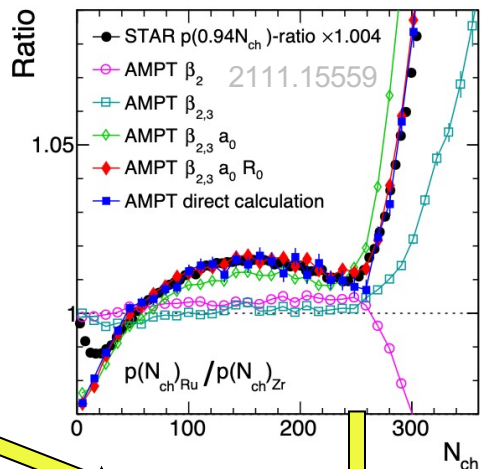
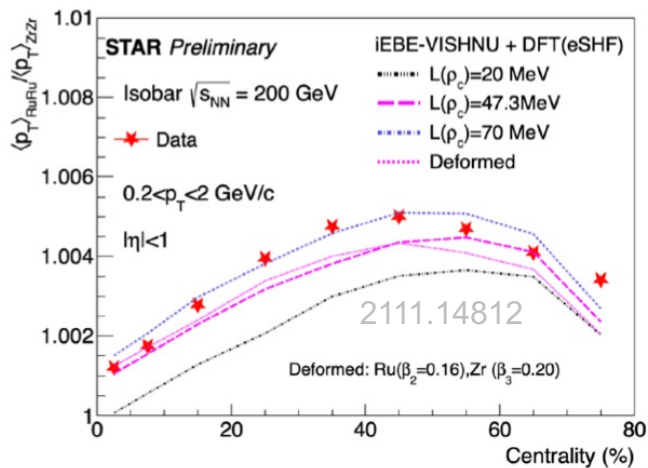
- $\beta_{2\text{Ru}} \sim 0.16$ increase v_2 , no influence on v_3 ratio
- $\beta_{3\text{Zr}} \sim 0.2$ decrease v_2 and v_3 ratio
- $\Delta a_0 = -0.06$ fm increase v_2 mid-central,
- Radius $\Delta R_0 = 0.07$ fm slightly affects v_2 and v_3 ratio.

Is ^{96}Zr octupole deformed?

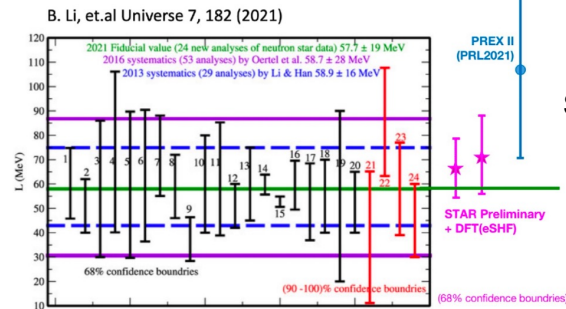


Imaging the radial structures

- Radial parameters R_0 , a_0 are properties of one-body distribution $\rightarrow \langle p_T \rangle$, $\langle N_{ch} \rangle$, $v_2^{RP} \sim v_2\{4\}$, σ_{tot}



Constrain neutron skin and symmetry energy

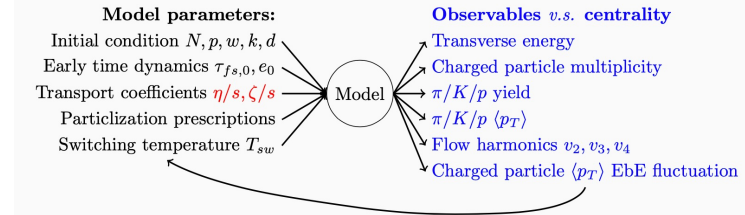


See talks of H. Xu, Z. Xu

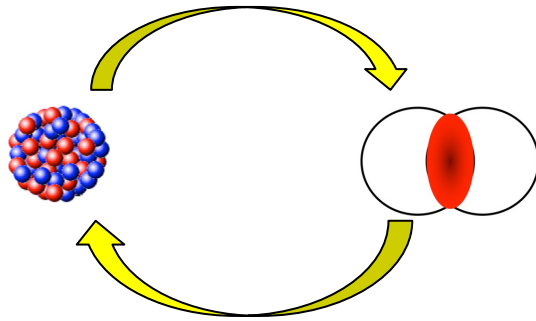
Opportunities

Low-energy: complexity & interpretation depend on location in nuclide chart
 High-energy: fast snapshot of nucleon distribution for any collision species.

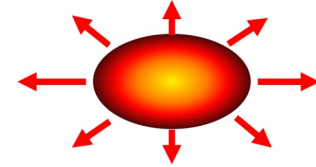
Current extraction of QGP properties are limited by the initial condition



constrain initial condition via nuclei with known structure



Better constraints on properties of QGP



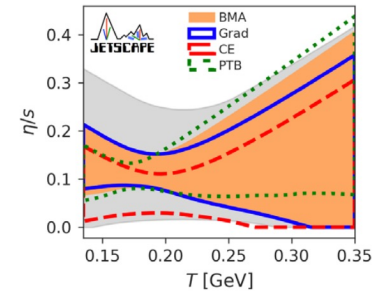
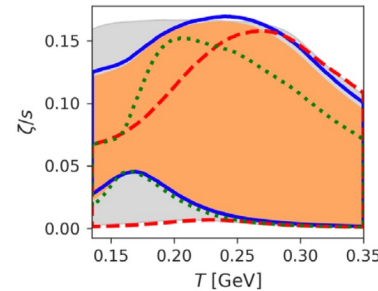
Constrain the structure for nuclei of interest with known initial condition

Systematic approaches for this purpose exist

Many potential applications

- 1) Odd mass nuclei
- 2) Higher-order deformations
- 3) Shape fluctuations/coexistence
- 4) Neutrinoless double-beta decay

...



How to obtain the shape of nuclei of interest

In central collisions

$$\langle \epsilon_2^2 \rangle = a' + b' \beta_2^2 \quad a' = \langle \epsilon_2^2 \rangle_{|\beta_2=0} \propto 1/A$$

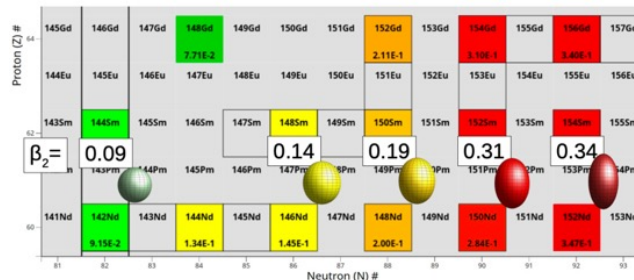
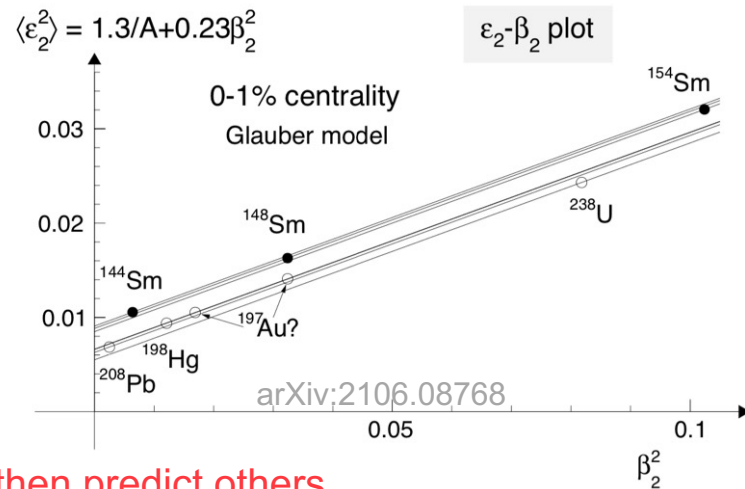
$$\langle v_2^2 \rangle = a + b \beta_2^2 \quad a = \langle v_2^2 \rangle_{|\beta_2=0} \propto 1/A$$

b' , b are \sim independent of system

Systems with similar A fall on the same curve.

Fix a and b with two isobar systems with known β_2 , then predict others.

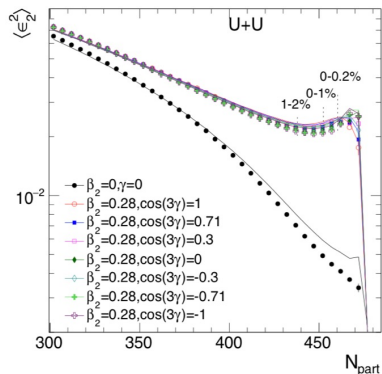
Transition from nearly-spherical to well-deformed nuclei when size increase by less than 7%. Using HI to access the multi-nucleon correlations leading to such shape evolution,



How to constrain triaxiality

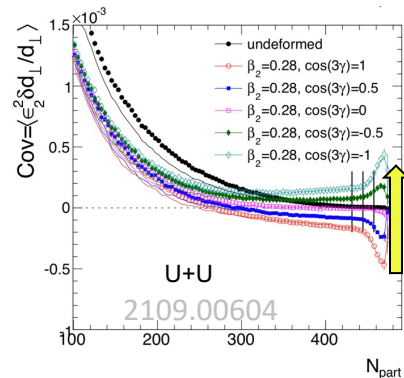
variances insensitive to γ

$$\langle v_2^2 \rangle \propto a + b\beta_2^2$$



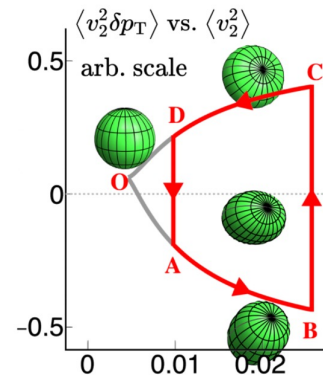
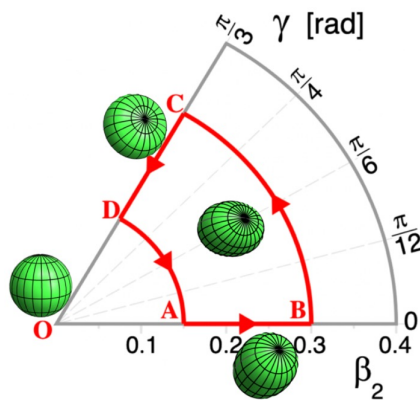
Skewness sensitive to γ

$$\langle v_2^2 \delta p_T \rangle \propto a - b \cos(3\gamma) \beta_2^3$$



Use variance to constrain β_2 , then use skewness to constrain γ

Map from (β_2, γ) plane to HI observables:

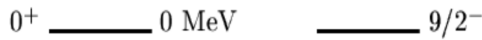


System scan to map out this trajectory: calibrate coefficients with species with known β, γ , then predict for species of interest.

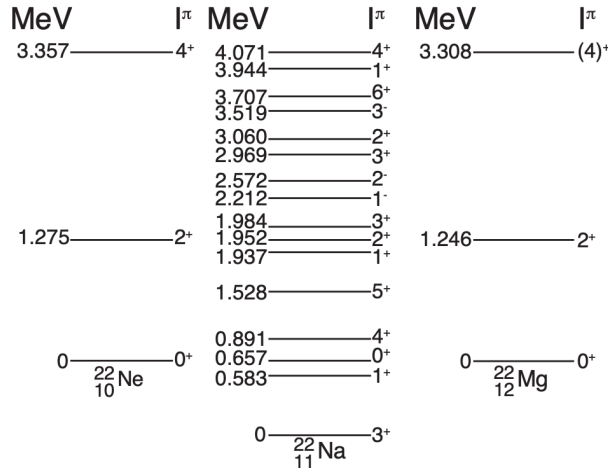
Odd N or Z nuclei



nuclear shape is often presumed to be similar to adjacent even-even nuclei.



their spectroscopic data are more complex e.g. by the coupling of the single unpaired nucleon with the nuclear core.



by comparing the flow observables of odd-mass nuclei to selected even-even neighbors with established shapes, the high-energy approach avoids this complication.

Higher-order deformations β_3 and β_4

Ratio of v_n in UCC region are mainly sensitive to β_n

Uranium 238

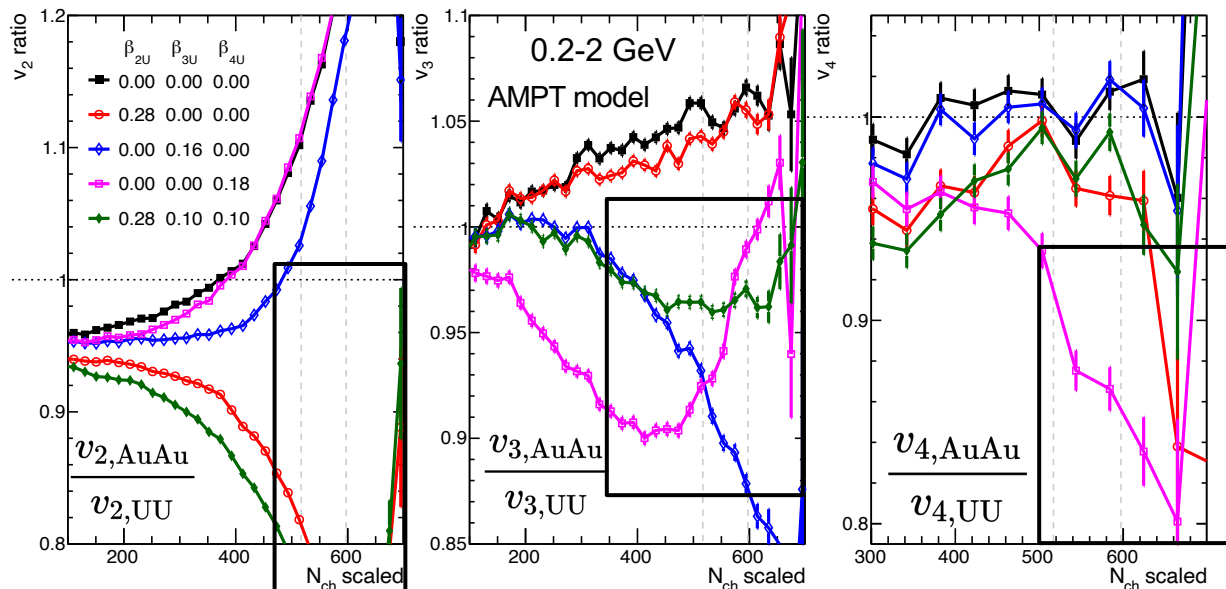
β_2	β_3	β_4
0.286[12]	0.078[13]	0.07 - 0.09[14, 15]

Expectation:

$$\langle v_2^2 \rangle \approx a_2 + b_{2,2}\beta_2^2 + b_{2,3}\beta_3^2$$

$$\langle v_3^2 \rangle \approx a_3 + b_{3,3}\beta_3^2 + b_{3,4}\beta_4^2$$

$$\langle v_4^2 \rangle \approx a_4 + b_{4,4}\beta_4^2$$



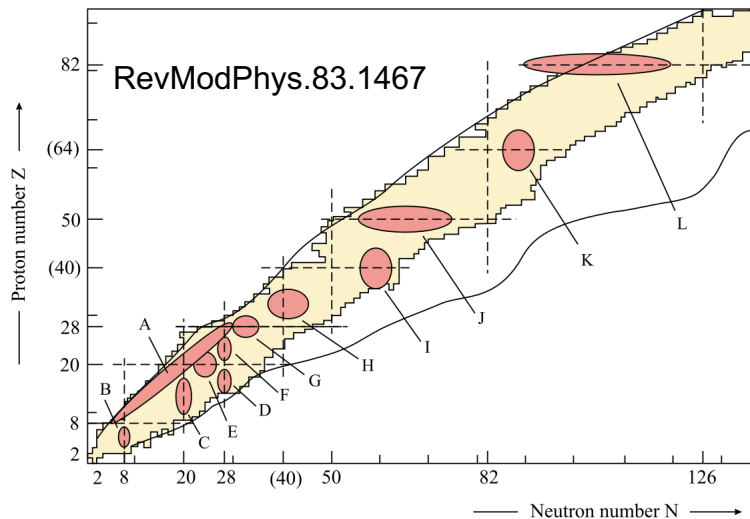
β_{4U} constrained using v_4 ratio in central region

order of v_3 reversed by considering non-zero $\beta_{3U} \beta_{4U}$

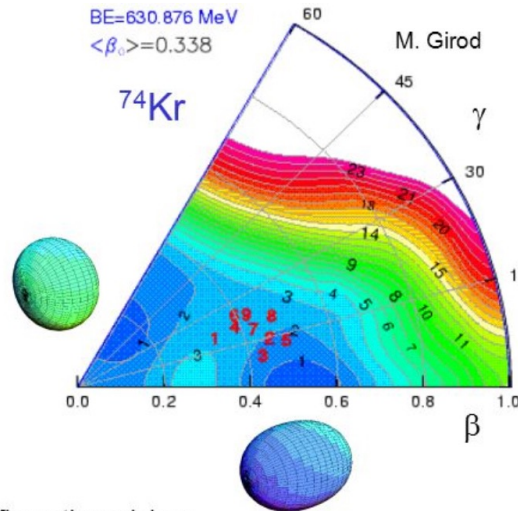
v_2 ratio is mostly affected by β_{2U} , but also β_{3U}

Shape fluctuation and coexistence

nuclei can have several low-lying states with different intrinsic shapes
 probe the shape entanglement?



Each collision picks out one shape component of the ground state WF



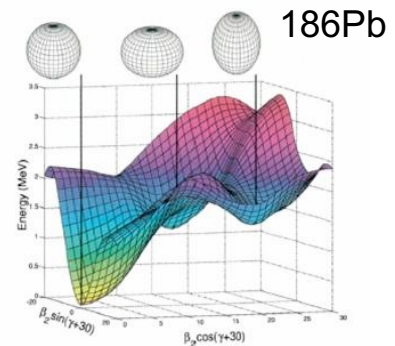
Configuration mixing:

$$|0_1^+\rangle = +\cos\eta |0_{\text{pro}}^+\rangle + \sin\eta |0_{\text{obl}}^+\rangle$$

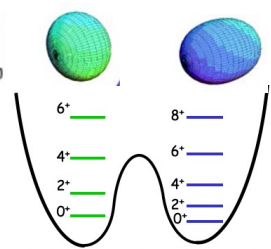
$$|0_2^+\rangle = -\sin\eta |0_{\text{pro}}^+\rangle + \cos\eta |0_{\text{obl}}^+\rangle$$

electric monopole (E0) transition

$$\langle 0_2^+ || \mathbf{M}(E0) || 0_1^+ \rangle \propto \sin\eta \cos\eta (\beta_{\text{pro}}^2 - \beta_{\text{obl}}^2)$$



Nature 405,430 (2000)

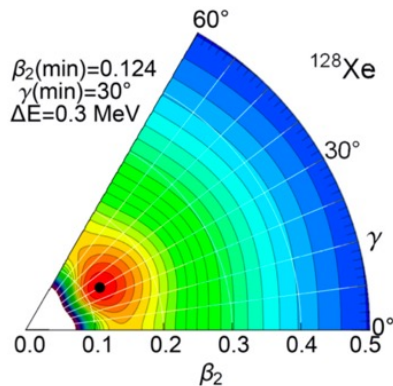
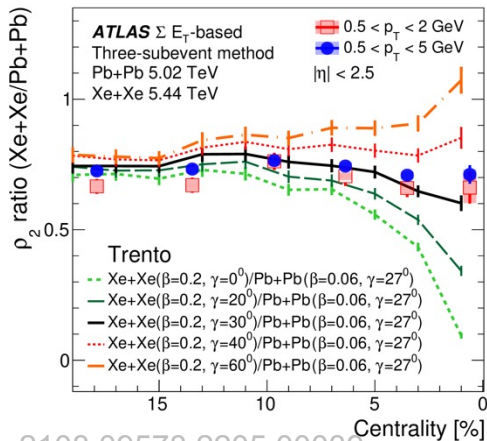


Shape fluctuations via high-order correlations.

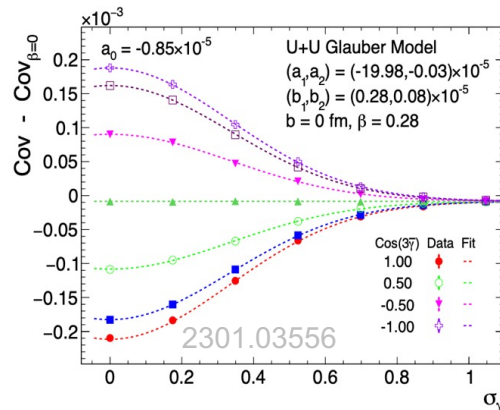
$$R = \frac{\langle v_2^2 \delta[p_T] \rangle_{129 Xe}}{\langle v_2^2 \delta[p_T] \rangle_{208 Pb}}$$

Large shape fluct., esp along γ

Fluctuation in γ washes out difference between prolate and oblate, such that all results approach triaxial case



$$\langle \cos(3\gamma) \rangle \approx e^{-\frac{9\sigma_\gamma^2}{2}} \cos(3\bar{\gamma})$$



Kumar sum rule

$$\langle \beta^2 \rangle = \frac{16\pi^2}{9A^2 R_0^4} \langle \hat{Q}^2 \rangle \quad \sigma \langle \beta^2 \rangle / \langle \beta^2 \rangle = \sigma \langle \hat{Q}^2 \rangle / \langle \hat{Q}^2 \rangle$$

2-p correlation

4-p correlation

$$\cos 3\gamma = -\sqrt{\frac{7}{2}} \frac{\langle \hat{Q}^3 \rangle}{\langle \hat{Q}^2 \rangle^{3/2}} \quad \frac{\sigma^2(\cos 3\gamma)}{(\cos 3\gamma)^2} = \frac{\sigma^2 \langle \hat{Q}^3 \rangle}{\langle \hat{Q}^3 \rangle^2} + \frac{9}{4} \frac{\sigma^2 \langle \hat{Q}^2 \rangle}{\langle \hat{Q}^2 \rangle^2} - 3 \frac{\langle \hat{Q}^5 \rangle - \langle \hat{Q}^3 \rangle \langle \hat{Q}^2 \rangle}{\langle \hat{Q}^3 \rangle \langle \hat{Q}^2 \rangle}$$

3-p correlation

6-p correlation

Heavy ion observables:

$$\frac{\langle \varepsilon_2^2 \rangle}{\frac{3}{4\pi} \langle \beta_2^2 \rangle} \quad \xleftrightarrow{\text{arXiv:2301.03556}} \quad \frac{\langle \varepsilon_2^4 \rangle - 2 \langle \varepsilon_2^2 \rangle^2}{-\frac{9}{112\pi^2} (7 \langle \beta_2^2 \rangle^2 - 5 \langle \beta_2^4 \rangle)}$$

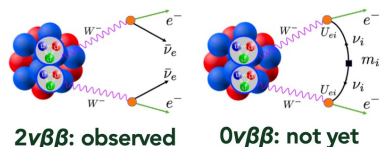
$$\frac{\langle \varepsilon_2^2 (\delta d_\perp / d_\perp) \rangle}{-\frac{3\sqrt{5}}{112\pi^{3/2}} \langle \cos(3\gamma) \beta_2^2 \rangle} \quad \xleftrightarrow{\quad} \quad \frac{(\langle \varepsilon_2^6 \rangle - 9 \langle \varepsilon_2^4 \rangle \langle \varepsilon_2^2 \rangle + 12 \langle \varepsilon_2^2 \rangle^3) / 4}{\frac{81}{256\pi^3} [\langle \beta_2^3 \rangle^3 - \frac{45}{14} \langle \beta_2^2 \rangle \langle \beta_2^4 \rangle - \frac{1175}{6006} \langle \beta_2^6 \rangle + \frac{25}{3003} \langle \cos(6\gamma) \beta_2^6 \rangle]}$$

2108.09578,2205.00039

PhysRevC.101.064318

2301.03556

Neutrinoless double-beta decay



$$[T_{1/2}^{0\nu}]^{-1} = G_{0\nu}(Q, Z) |M_{0\nu}|^2 \langle m_{\beta\beta} \rangle^2$$

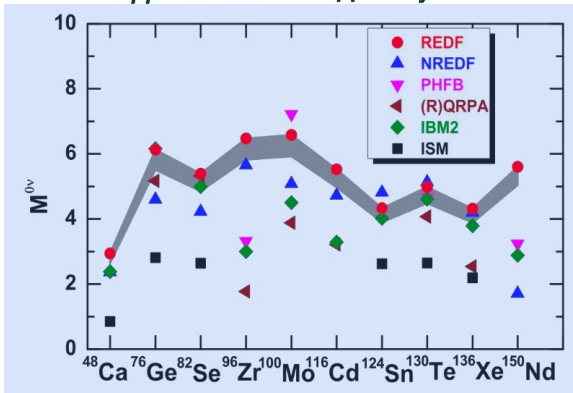
Nuclear matrix element

Need to know the overlap of nuclear wavefunction between initial nuclei and its final isobar nuclei.

x2-3 difference in matrix element leads to x10 change in lifetime

Challenge: modeling nucleon correlations in nuclear structure including quadruple and pairing correlations

HI collision could measure structure differences precisely



Talks by CF Jiao, J.M Yao

Potassium 19 K 39.098	Calcium 20 Ca 40.078	Scandium 21 Sc 44.956	Titanium 22 Ti 47.867	Vanadium 23 V 50.942	Chromium 24 Cr 51.996	Manganese 25 Mn 54.938	Iron 26 Fe 55.845(2)	Cobalt 27 Co 58.933	Nickel 28 Ni 58.693	Copper 29 Cu 63.546(3)	Zinc 30 Zn 65.38(2)	Gallium 31 Ga 69.723	Germanium 32 Ge 72.630(8)	Arsenic 33 As 74.922	Selenium 34 Se 78.971(8)	Bromine 35 Br 79.904	Krypton 36 Kr 83.798(2)
Rubidium 37 Rb 85.468	Strontium 38 Sr 87.62	Yttrium 39 Y 88.906	Zirconium 40 Zr 91.224(2)	Niobium 41 Nb 92.906(2)	Molybdenum 42 Mo 95.94	Technetium 43 Tc 98.906	Ruthenium 44 Ru 101.07(2)	Rhodium 45 Rh 102.91	Palladium 46 Pd 106.42	Silver 47 Ag 107.87	Cadmium 48 Cd 112.41	Indium 49 In 114.82	Tin 50 Sn 118.710	Antimony 51 Sb 121.76	Te 52 Te 127.603(3)	Iodine 53 I 126.90	Xenon 54 Xe 131.29
Cesium 55 Cs 132.91	Barium 56 Ba 137.33	Lanthanum 57-70 * Lu 174.97	Hafnium 72 Hf 178.49(2)	Tantalum 73 Ta 180.95	Tungsten 74 W 183.84	Rhenium 75 Re 186.21	Osmium 76 Os 190.23(2)	Iridium 77 Ir 192.22	Pt 78 Pt 195.08	Au 79 Au 196.97	Hg 80 Hg 200.59	Tl 81 Tl 204.38	Pb 82 Pb 207.2	Bi 83 Bi 208.98	Po 84 Po [209]	At 85 At [209.99]	Rn 86 Rn [222.02]
Francium 87 Fr [223.02]	Radium 88 Ra [226.03]	Actinoids 89-102 ** Lr [262.11]	Rf 104 Rf [267.12]	Db 105 Db [269.13]	Sg 106 Sg [269.13]	Bh 107 Bh [270.13]	Hs 108 Hs [270.13]	Mt 109 Mt [278.16]	Ds 110 Ds [281.17]	Rg 111 Rg [281.17]	Cn 112 Cn [285.18]	Nh 113 Nh [286.18]	Fl 114 Fl [289.19]	Mc 115 Mc [289.19]	Lv 116 Lv [293.20]	Ts 117 Ts [293.21]	Og 118 Og [294.21]

*lanthanoids

Lanthanum 57 La 138.91	Cerium 58 Ce 140.12	Praseodymium 59 Pr 140.91	Neodymium 60 Nd 144.24	Promethium 61 Pm [144.91]	Samarium 62 Sm 150.36(2)	Europium 63 Eu 151.96	Gadolinium 64 Gd 157.25(3)	Terbium 65 Tb 158.93	Dysprosium 66 Dy 162.50	Holmium 67 Ho 164.93	Erbium 68 Er 167.26	Thulium 69 Tm 168.93	Ytterbium 70 Yb 173.05
---------------------------------	------------------------------	------------------------------------	---------------------------------	------------------------------------	-----------------------------------	--------------------------------	-------------------------------------	-------------------------------	----------------------------------	-------------------------------	------------------------------	-------------------------------	---------------------------------

Summary

- Nuclear structure imaging could be a discovery tool for nuclear structure and high-energy nuclear physics
- High- and low-energy techniques together enable study of evolution of nuclear structure across energy and time scales.
- Future research could leverage collider facilities to conduct experiments with selected isobaric or isobar-like pairs

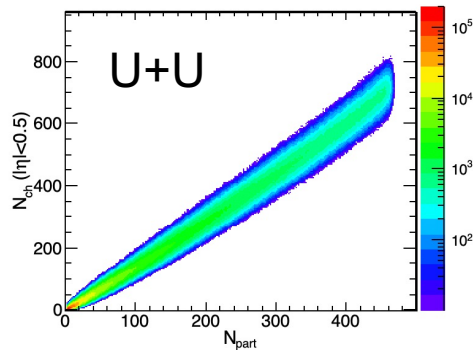
2102.08158

A	isobars	A	isobars	A	isobars	A	isobars	A	isobars	A	isobars
36	Ar, S	80	Se, Kr	106	Pd, Cd	124	Sn, Te, Xe	148	Nd, Sm	174	Yb, Hf
40	Ca, Ar	84	Kr, Sr, Mo	108	Pd, Cd	126	Te, Xe	150	Nd, Sm	176	Yb, Lu, Hf
46	Ca, Ti	86	Kr, Sr	110	Pd, Cd	128	Te, Xe	152	Sm, Gd	180	Hf, W
48	Ca, Ti	87	Rb, Sr	112	Cd, Sn	130	Te, Xe, Ba	154	Sm, Gd	184	W, Os
50	Ti, V, Cr	92	Zr, Nb, Mo	113	Cd, In	132	Xe, Ba	156	Gd, Dy	186	W, Os
54	Cr, Fe	94	Zr, Mo	114	Cd, Sn	134	Xe, Ba	158	Gd, Dy	187	Re, Os
64	Ni, Zn	96	Zr, Mo, Ru	115	In, Sn	136	Xe, Ba, Ce	160	Gd, Dy	190	Os, Pt
70	Zn, Ge	98	Mo, Ru	116	Cd, Sn	138	Ba, La, Ce	162	Dy, Er	192	Os, Pt
74	Ge, Se	100	Mo, Ru	120	Sn, Te	142	Ce, Nd	164	Dy, Er	196	Pt, Hg
76	Ge, Se	102	Ru, Pd	122	Sn, Te	144	Nd, Sm	168	Er, Yb	198	Pt, Hg
78	Se, Kr	104	Ru, Pd	123	Sb, Te	146	Nd, Sm	170	Er, Yb	204	Hg, Pb

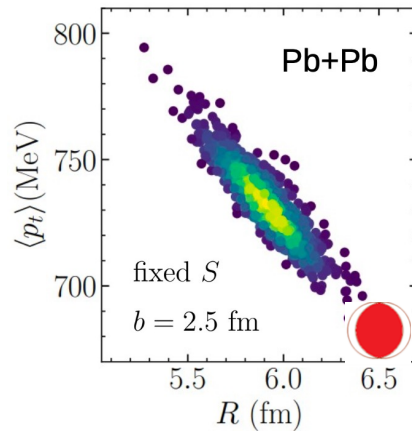


Correlation between initial and final state

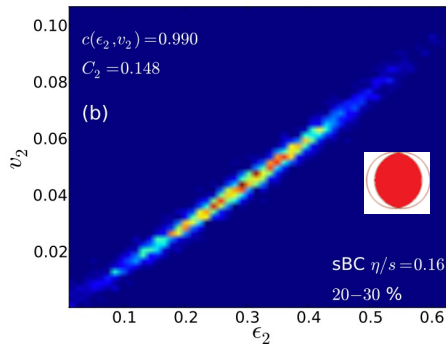
$$N_{ch} \propto N_{part}$$



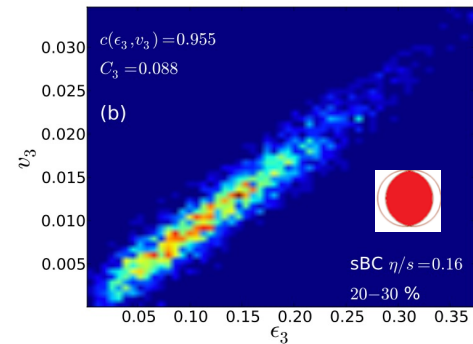
$$\frac{\delta[p_T]}{[p_T]} \propto -\frac{\delta R_{\perp}}{R_{\perp}}$$



$$V_2 \propto \mathcal{E}_2$$

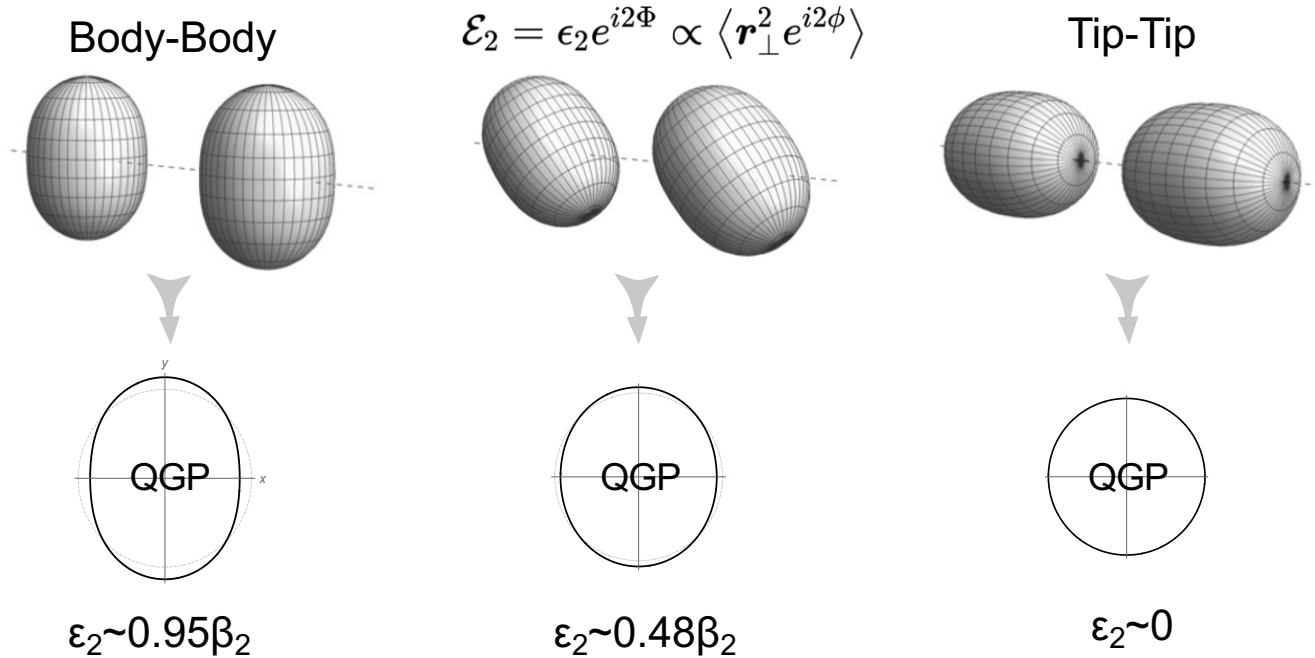


$$V_3 \propto \mathcal{E}_3$$



Nice correlation at very high energy

Connecting initial condition to nuclear shape



$$\epsilon_2 = \underbrace{\epsilon_0}_{\text{undeformed}} + \underbrace{p(\Omega_1, \Omega_2)}_{\text{phase factor}} \beta_2 + \mathcal{O}(\beta_2^2)$$



$$\langle \epsilon_2^2 \rangle \approx \langle \epsilon_0^2 \rangle + 0.2\beta_2^2$$

Shape depends on Euler angle $\Omega = \varphi\theta\psi$

Sensitivity to other structure parameters

In ultra-central collisions, ratios are controlled by β_{2U} and γ_U .

In non-central collisions, v_2 ratio is sensitive to nuclear skin

